

01

## Emission spectra of molecular gases $\text{CHF}_3$ , $\text{CCl}_2\text{F}_2$ , $\text{SF}_6$ in the range 3–20 nm under pulsed laser excitation using various gas jets as targets

© V.E. Guseva<sup>1</sup>, A.N. Nechay<sup>2¶</sup>, A.A. Perekalov<sup>2</sup>, N.N. Salashchenko<sup>2</sup>, N.I. Chkhalo<sup>2</sup>

<sup>1</sup>Lobachevsky State University,  
603950 Nizhny Novgorod, Russia

<sup>2</sup>Institute of Physics of Microstructures, Russian Academy of Sciences,  
603087 Nizhny Novgorod, Russia

¶ e-mail: nechay@ipm.sci-nnov.ru

Received September 28, 2021

Revised October 21, 2021

Accepted November 01, 2021

The article considers the results of studies of the emission spectra of  $\text{CHF}_3$ ,  $\text{CCl}_2\text{F}_2$ ,  $\text{SF}_6$  upon excitation by pulsed laser radiation. We used Nd:YAG laser,  $\lambda = 1064 \text{ nm}$ ,  $\tau = 5 \text{ ns}$ , and  $E_{\text{pulse}} = 0.8 \text{ J}$ . The spectral range of 3–20 nm was studied. We used capillary and supersonic conical nozzles with  $d_{\text{crit}} = 145 \mu\text{m}$ ,  $2\alpha = 12^\circ$ ,  $L = 5 \text{ mm}$ , and  $d_{\text{crit}} = 450 \mu\text{m}$ ,  $2\alpha = 11^\circ$ ,  $L = 5 \text{ mm}$  to form an atomic cluster beam. The emission spectra for various gas targets were obtained, the obtained spectra were deciphered, and the ions emitting in this spectral range were determined. We observed that with increasing particle concentration in the zone of laser spark, the radiation intensity increases. In this case, the intensity of ion lines with high degrees of ionization increases faster.

**Keywords:** cluster beams, extreme ultraviolet radiation, emission spectra, laser spark, x-ray spectrometer-monochromator.

DOI: 10.21883/EOS.2022.02.53209.2771-21

### Introduction

Currently, studies are actively developing in the field of short-wavelength, in particular, soft X-ray and extreme ultraviolet radiation (MXR and EUV). Previously, studies in the MXR and EUV ranges using multilayer optics were associated with laboratory and space plasma diagnostics [1], problems of short-wavelength projection lithography [2]. Currently, laboratory applications using the MXR and EUV range techniques are coming to the fore. In particular, these are studies related to the study of the structure and ordering of nanoobjects of both natural and artificial origin. In this direction one can single out X-ray microscopy and studies of the multilayer nanofilm structure [3,4].

For laboratory purposes, plasma sources have found the greatest application, including those in which plasma is created by pulsed laser radiation (laser-plasma sources (LPS)) [5–7]. Gas jets [5,8], solid-state [9,10] and frozen gas targets [11,12] are used as targets for pulsed excitation.

Previously, we have studied the emission properties of inert gases using various systems for formation of gas targets [13–15]. In this article, these studies are continued, the emission properties of molecular gases, including fluorine, chlorine, and sulfur, are investigated.

### Research plant

The plant described in detail in [16] was used for research. The plant operated as follows. The gas under study enters a conical convergent-divergent nozzle, and gas target

is formed when flowing out of this nozzle into vacuum volume. Pumping is carried out by cryocondensation and cryoadsorption pumps. The laser radiation is directed to a short-focus lens, in the focus of which breakdown occurs and plasma is formed. Polychromatic MXR and EUV radiation of the plasma, passing through a free-hanging X-ray filter, is directed to the input mirror of the spectrometer-monochromator RSM-500. Then monochromatic MXR and EUV radiation is detected by a pulsed detector.

To excite the gas jet, NL300 Series Nd:YAG Laser was used with the following parameters: wavelength 1064 nm, laser pulse energy 0.8 J, pulse duration 5.2 ns, frequency up to 10 Hz. Laser radiation is focused on a gas target using a lens with a focal length of 45 mm. The calculated focal spot diameter is 66  $\mu\text{m}$ . A free-hanging Mo/ZrSi<sub>2</sub> filter with layer thicknesses in a bilayer of 1.5/2.5 nm is used, the number of bilayers is 12. Also, a free-hanging filter is also a protection against particles of various nature, formed during the operation of the MXR and EUV radiation source.

The emission spectra were recorded using a spectrometer-monochromator RSM-500. The curvature radius of the input mirror is 4 m, that of the grating - 3 m, the number of lines is 600 lines/mm. The used spherical mirrors and gratings were made of K-8 glass coated with gold. These mirrors and gratings were supplied with the RSM-500 device. The spectral resolution of the device, measured at the  $L$ -absorption edges of silicon and aluminum free-hanging filters and  $K$ -edge of beryllium free-hanging filters, as well as at the zero-order half-width, was 0.04 nm. For the gratings and mirrors used, the studied wavelength range was 3–20 nm.

The following nozzles were used to form gas jet targets: a small conical convergent-divergent nozzle with  $d_{cr} = 145 \mu\text{m}$ ,  $2\alpha = 12^\circ$ ,  $L = 5 \text{ mm}$ , a large conical convergent-divergent nozzle with  $d_{cr} = 450 \mu\text{m}$ ,  $2\alpha = 11^\circ$ ,  $L = 5 \text{ mm}$  and a capillary with a diameter of  $d = 500 \mu\text{m}$ . These gas jet formation systems have the following features.

A conical convergent-divergent nozzle of small critical section ( $d_{cr} = 145 \mu\text{m}$ ) forms a directed supersonic gas jet. When a cooled gas or gas under high pressure is supplied, a narrowly directed cluster beam is formed with a large proportion of condensate in it. These nozzles can be used at various temperatures and pressures of the supplied gas in the presence of pumping systems of acceptable power ( $\sim 1000 \text{ l/s}$ ). As a rule, these nozzles are used to form cluster beams in a constant gas outflow regime and are convenient when using laser systems with a high pulse repetition rate.

A conical convergent-divergent nozzle of large critical section ( $d_{cr} = 450 \mu\text{m}$ ) also forms a directed supersonic gas jet. But a large critical section leads to high gas flow rates, which, with pumping systems of acceptable power ( $\sim 1000 \text{ l/s}$ ), requires the use of a pulse valve. In turn, the use of high-speed pulse valves limits the pressure ranges, and especially gas temperature ranges at the nozzle inlet, and does not allow the cluster beams with a large cluster size to be obtained. Also, the use of pulse valves leads to the need to use laser systems with a low  $\sim 10 \text{ Hz}$  pulse repetition rate.

A capillary with a large section  $d = 500 \mu\text{m}$  is characterized by the sonic regime of gas outflow and forms a gas cloud with an almost isotropic gas expansion in all directions from the capillary cutoff. The large diameter of the capillary used leads to high gas flow rates, which also requires the use of a pulse valve for pumping systems of acceptable power ( $\sim 1000 \text{ l/s}$ ). At the same time, this system for forming a gas-jet target is the simplest and most reliable.

Gas jets formed in the process of outflow from conical nozzles into vacuum generally have a complex spatial structure determined by the gas parameters at the nozzle inlet and the geometrical parameters of the nozzles. Particularly difficult are the problems of describing atomic-cluster jets formed by outflow of condensing gas from convergent-divergent nozzles into vacuum. The gas-dynamic calculation of the structure of such an atomic cluster target is very time consuming and is a separate problem. In our article, on the basis of [5], it is assumed that the concentration of particles in gas jets is  $\sim 10^{19} \text{ mol/cm}^3$ .

## Results

### Studies of gas-jet targets based CHF<sub>3</sub>

Trifluoromethane CHF<sub>3</sub> is heavy molecular gas with low reactivity under experimental conditions, characterized by a line emission spectrum with high-intensity lines in the MXR and EUV regions of the spectrum. Ease of pumping, satisfactory thermodynamic properties, and availability make

**Table 1.** Emission lines of fluorine ions in the spectrum of the CHF<sub>3</sub> targets

Wavelength nm	Intensity, rel. units	Ion	Transition
7.83	180	F VII	$1s^2 2s - 1s^2 5p$
8.12	180	F VII	$1s^2 2p - 1s^2 6d$
8.58	510	F VII	$1s^2 2p - 1s^2 5d$
8.64	490	F VII	$1s^2 2s - 1s^2 4p$
9.57	1700	F VII	$1s^2 2p - 1s^2 4d$
9.73	170	F VII	$1s^2 2p - 1s^2 4s$
9.91	200	F VI	$1s^2 2s 2p - 1s^2 2s 5d$ [21]
10.89	550	F VI	$1s^2 2s 2p - 1s^2 2s 4d$
11.294	3050	F VII	$1s^2 2s - 1s^2 3p$
11.298	600	F VII	$1s^2 2s - 1s^2 3p$
11.47	230	F VI	$1s^2 2s^2 - 1s^2 2p 3s$
11.6	130	F VI	$1s^2 2p^2 - 1s^2 2p 4d$ [21]
12.01	250	F VI	$1s^2 2s 2p - 1s^2 2p 3p$ [21]
12.21	600	F VI	$1s^2 2s 2p - 1s^2 2p 3p$ [21]
12.31	220	F VI	$1s^2 2s 2p - 1s^2 2p 3p$
12.44	560	F VI	$1s^2 2s 2p - 1s^2 2p 3d$
12.69	1000	F VI	$1s^2 2s^2 - 1s^2 2p 3p$
12.78	8900	F VII	$1s^2 2p - 1s^2 3d$
13.25	650	F V	$1s^2 2s 2p^2 - 1s^2 2s 2p 4d$ [21]
13.48	1590	F VII	$1s^2 2p - 1s^2 3s$
13.70	100	F VI	$1s^2 2s 2p - 1s^2 2s 3d$
13.99	3100	F VI	$1s^2 2s 2p - 1s^2 2s 3d$
14.59	1200	F VI	$1s^2 2p^2 - 1s^2 2p 3d$
14.68	2350	F VI	$1s^2 2p^2 - 1s^2 2p 3d$
14.87	900	F VI	$1s^2 2p^2 - 1s^2 2p 3d$
15.25	300	F V	$1s^2 2s^2 2p - 1s^2 2s 2p 3p$ [21]
15.38	750	F VI	$1s^2 2s 2p - 1s^2 2s 3s$
15.45	300	F VI	$1s^2 2p^2 - 1s^2 2p 3d$
15.62	750	F VI	$1s^2 2s 2p - 1s^2 2s 3d$
15.85	310	F V	$1s^2 2s 2p^2 - 1s^2 2s 2p 3d$
16.15	310	F VI	$1s^2 2p^2 - 1s^2 2p 3s$
16.31	550	F VI	$1s^2 2p^2 - 1s^2 2p 3d$
16.35	980	F VI	$1s^2 2p^2 - 1s^2 2p 3s$
16.74	580	F VI	$1s^2 2s^2 2p - 1s^2 2s^2 3d$
17.12	150	F V	$1s^2 2p^3 - 1s^2 2p^2 3d$
17.31	350	F VI	$1s^2 2s 2p - 1s^2 2s 3s$
17.5	350	F VII	$1s^2 3s - 1s^2 9p$
17.59	170	F V/F VI	—
17.86	400	F V	$1s^2 2p^3 - 1s^2 2p^2 3d$
18.48	160	F VII	$1s^2 3p - 1s^2 9d$
18.83	250	F VI	$1s^2 2p^2 - 1s^2 2p 3s$
19.48	800	F VII	$1s^2 3d - 1s^2 8p$

CHF<sub>3</sub> one of the most promising gas targets. Fluorine was previously studied in [17,18] as targets for MXR and EUV radiation LPS.

Figure 1 shows the CHF<sub>3</sub> emission spectra measured using a capillary and a cone nozzle with throat of  $450 \mu\text{m}$  at the following gas parameters: gas pressure at the nozzle inlet 3 bar, gas temperature 300 K.

The studied spectral range was 3–20 nm. The radiation intensity is given in relative units. One can see a number

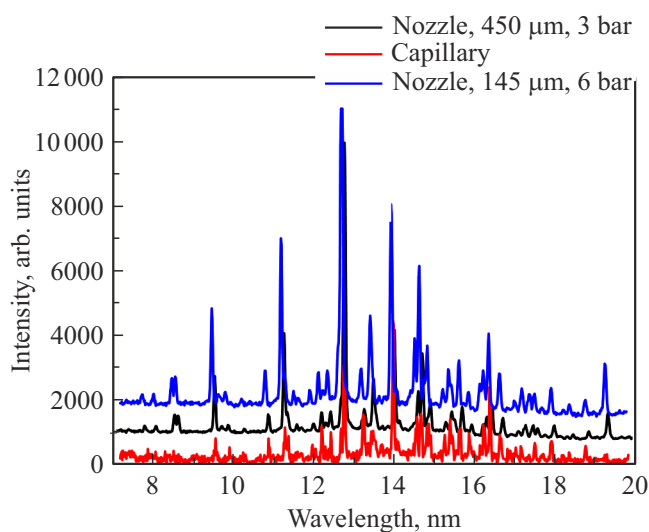


**Figure 1.** Emission spectra of  $\text{CHF}_3$  targets using a capillary, a cone nozzle with  $d_{\text{cr}} = 450 \mu\text{m}$  and a cone nozzle with  $d_{\text{cr}} = 145 \mu\text{m}$  as a jet source.

of intense lines within the range of 8–20 nm, formed by transitions on F V, F VI, F VII ions. Lines of carbon ions are not observed in the studied spectral range. It can be seen from the figure that the use of a convergent-divergent nozzle with  $d_{\text{cr}} = 450 \mu\text{m}$  leads to significant redistribution of the intensities of the fluorine emission lines with an increase in the line intensities at high ionization degrees (F VII). For short wavelengths, an increase in the noise component is observed, which occurs due to the features of the spectral device used.

The interpretation of the observed lines was carried out in accordance with [19–21] by comparing the spectra measured on different targets and is given in Table 1. A number of lines were observed in accordance with [21], but the transitions corresponding to them could not be established.

The relative line intensities for the spectra measured using gaseous  $\text{CHF}_3$  targets formed by outflow from various nozzles are given in Table 2. The line intensities were normalized to the line 12.78 nm (F VII), which made it possible to negate the change in the concentrations of fluorine ions in the discharge zone due to different gas dynamics of jet targets. In this table, the concentration of particles in the laser spark zone indirectly increases in the series of capillary–nozzle 145  $\mu\text{m}$  (3 bar)–nozzle 450  $\mu\text{m}$  (3 bar)–nozzle 145  $\mu\text{m}$  (6 bar). An exact concentration calculation was not carried out, since it is a very complex problem of gas dynamics associated with condensation in supersonic gas jets.

Based on the data given in Table 2, the following conclusions can be drawn.

With an increase in the particle concentration in the discharge zone, a relative growth of lines corresponding to ions of high degrees of ionization (F VII) is observed, which corresponds to an increase in plasma temperature.

The change in the relative line intensities is quite large, up to 8 times. At the same time, the observed change in plasma temperature does not lead to the appearance of fluorine ions with other ionization degrees. This can be explained by the fact that the power of the laser system used is insufficient for the formation of F VIII ions.

The highest plasma temperature is observed when using a nozzle with a critical section of 145  $\mu\text{m}$  at a pressure of 6 bar. High concentrations of particles in the discharge zone and high plasma temperatures in this case can be explained by high condensation temperature of  $\text{CHF}_3$  and, accordingly, formation of condensate in the jet during gas outflow into vacuum volume.

A separate experiment was carried out to study cooled  $\text{CHF}_3$  jets. It was found that the emission spectra for the 145  $\mu\text{m}$  nozzle, when the gas is cooled at the nozzle inlet ( $T = 216 \text{ K}$ ,  $p = 3 \text{ bar}$ ), are almost identical to the emission spectra obtained at increased pressure ( $T = 300 \text{ K}$ ,  $p = 6 \text{ bar}$ ), which indicates a developed condensation process in both cases.

### Studies of gas-jet targets based $\text{SF}_6$

Sulfur hexafluoride  $\text{SF}_6$  is heavy molecular gas with low reactivity under experimental conditions, characterized by a line emission spectrum with high-intensity lines in the MXR and EUV regions of the spectrum. Ease of pumping, satisfactory thermodynamic properties, and availability also make  $\text{SF}_6$  a very promising gas target. This gas was previously studied in [22,23] as targets for MXR and EUV radiation LPS.

Figure 2 shows the  $\text{CHF}_3$  and  $\text{SF}_6$  emission spectra measured using a cone nozzle with throat of 450  $\mu\text{m}$  at the following gas parameters: pressure at the nozzle inlet 3 bar, gas temperature 300 K.

The studied spectral range was 3–20 nm. The radiation intensity is given in relative units. One can see a number of intense lines within the range of 8–20 nm, formed by transitions on F V, F VI, F VII ions. Against this

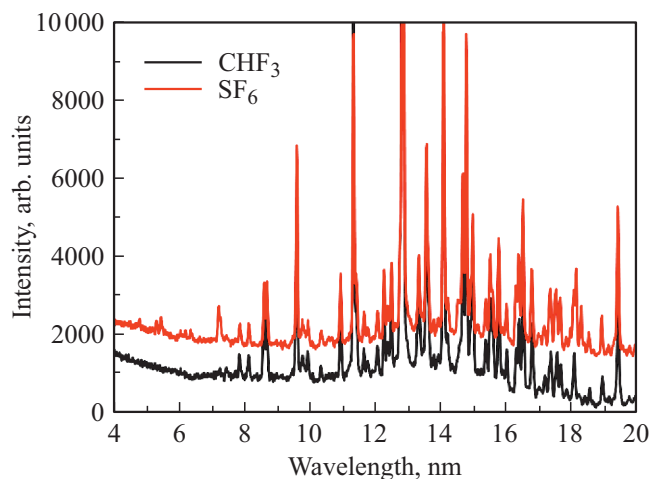


**Figure 2.** Emission spectra of  $\text{SF}_6$  and  $\text{CHF}_3$  targets using a cone nozzle with  $d_{\text{cr}} = 450 \mu\text{m}$  as a jet source.

**Table 2.** Relative intensities of fluorine ion lines in the CHF<sub>3</sub> target spectrum using different target formation systems

Wavelength, nm	Ion	Intensity for different targets			
		Capillary 500 μm, 3 bar	Nozzle 450 μm, 3 bar	Nozzle 145 μm, 3 bar	Nozzle 145 μm, 6 bar
9.57	F VII	0.26	0.19	0.17	0.33
10.89	F VI	0.25	0.06	0.08	0.11
11.294	F VII	0.36	0.34	0.34	0.57
12.21	F VI	0.36	0.07	0.07	0.11
12.44	F VI	0.31	0.07	0.08	0.11
12.78	F VII	1.00	1.00	1.00	1.00
13.25	F V	0.46	0.08	0.08	0.11
13.48	F VII	0.28	0.18	0.18	0.29
13.99	F VI	1.46	0.35	0.46	0.67
14.6	F VI	0.43	0.14	0.14	0.22
14.7	F VI	0.46	0.27	0.31	0.47
14.87	F VI	0.36	0.11	0.12	0.20
15.25	F V	0.24	0.03	0.03	0.06
15.38	F VI	0.41	0.07	0.09	0.13
15.62	F VI	0.31	0.09	0.11	0.16
16.15	F VI	0.15	0.04	0.05	0.09
16.31	F VI	0.36	0.06	0.09	0.14
16.35	F VI	0.77	0.10	0.18	0.26
16.74	F VI	0.26	0.06	0.10	0.12
17.86	F V	0.22	0.04	0.06	0.09
18.83	F VI	0.17	0.02	0.04	0.05
19.48	F VII	0.08	0.09	0.10	0.17

background, in the range 4–7 nm and ~ 18 nm, there are a number of lines of sulfur ions S VII and S VIII. There are no lines of carbon ions. For short wavelengths, an increase in the noise component is observed, which occurs due to the features of the spectral device used.

Based on comparison of the spectra of CHF<sub>3</sub> and SF<sub>6</sub>, a number of lines were identified that correspond to sulfur ions. It should be especially noted that in the range 11–17 nm, intense lines of sulfur ions are possible, which were not separated due to superposition on the fluorine ions lines. The interpretation of the observed lines was carried out in accordance with [19,20,24] and is given in Table 3. The interpretation faced a number of difficulties, since the emission spectra of sulfur in the MXR and EUV ranges are relatively little studied. Lines 15, 17.96, 18.1 nm, which have a relatively high intensity, have not been identified.

### Studies of gas-jet targets based CCl<sub>2</sub>F<sub>2</sub>

Dichlorodifluoromethane CCl<sub>2</sub>F<sub>2</sub> is heavy molecular gas with low reactivity under experimental conditions, characterized by a line emission spectrum with high-intensity lines in the MXR and EUV region of the spectrum. Ease of pumping, satisfactory thermodynamic properties, and availability make CCl<sub>2</sub>F<sub>2</sub> one of the interesting gas targets. As far as the authors know, this gas has not been studied as targets for MXR and EUV radiation LPS.

Figure 3 shows the CHF<sub>3</sub> and CCl<sub>2</sub>F<sub>2</sub> emission spectra measured using a cone nozzle with throat of 450 μm at the

**Table 3.** Emission lines of sulfur ions upon excitation of the SF<sub>6</sub> target

Wavelength, nm	Intensity, rel. units	Ion	Transition
4.64	200	S VIII	2s <sup>2</sup> 2p <sup>5</sup> –2s <sup>2</sup> 2p <sup>4</sup> 4s
5.14	300	S VIII	2s <sup>2</sup> 2p <sup>5</sup> –2s <sup>2</sup> 2p <sup>4</sup> 3d
5.30	400	S VIII	2s <sup>2</sup> 2p <sup>5</sup> –2s <sup>2</sup> 2p <sup>4</sup> 3d
6.18	200	S VIII	2s <sup>2</sup> 2p <sup>5</sup> –2s <sup>2</sup> 2p <sup>4</sup> 3s
6.33	300	S VIII	2s <sup>2</sup> 2p <sup>5</sup> –2s <sup>2</sup> 2p <sup>4</sup> 3s
7.20	900	S VII	2s <sup>2</sup> 2p <sup>6</sup> –2s <sup>2</sup> 2p <sup>5</sup> 3s
7.26	600	S VII	2s <sup>2</sup> 2p <sup>6</sup> –2s <sup>2</sup> 2p <sup>5</sup> 3s
15.16	400	*	*
18.16	2100	*	*
18.31	1200	*	*

Note.\* Emitting ions and transitions corresponding to these emission lines could not be established.

following gas parameters: pressure at the nozzle inlet 3 bar, gas temperature 300 K.

The studied spectral range was 3–20 nm. The radiation intensity is given in relative units. One can see a number of intense lines within the range of 8–20 nm, formed by transitions on F V, F VI, F VII ions. Against this background, in the range 6–7 nm and 16–19 nm, there are a number of lines of chlorine ions. There are no lines of carbon ions. For short wavelengths, an increase in the noise

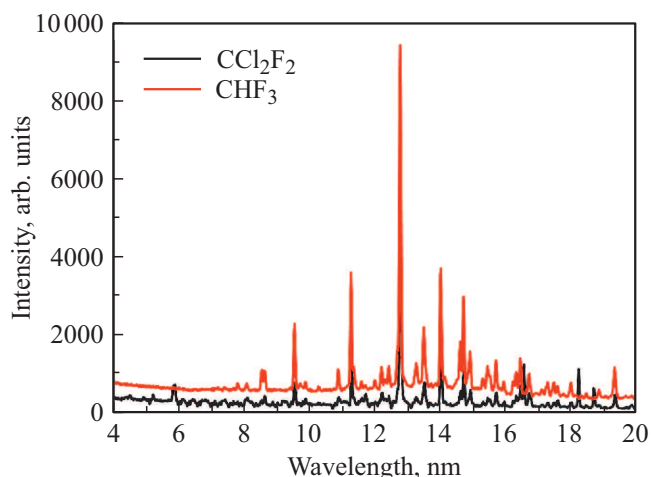


**Figure 3.** Emission spectra of CCl<sub>2</sub>F<sub>2</sub> and CHF<sub>3</sub> targets using a cone nozzle with  $d_{cr} = 450 \mu\text{m}$  as a jet source.

**Table 4.** Chlorine ion emission lines

Wavelength, nm	Intensity, rel. units	Ion	Transition
4.46	100	Cl VIII	$2p^6-2p^54s$
4.95	60	Cl VIII	$2p^6-2p^53d$
5.29	140	Cl VIII	$2p^6-2p^53d$
5.87	400	Cl VIII	$2p^6-2p^53s$
16.57	1100	Cl VIII	$2p^53s-2p^54p$
18.25	1000	Cl VIII	$2p^63p-2p^54d$
18.64	500	Cl VIII	$2p^63p-2p^54d$

component is observed, which occurs due to the features of the spectral device used.

Based on comparison of the spectra of CHF<sub>3</sub> and CCl<sub>2</sub>F<sub>2</sub>, a number of lines were identified that correspond to Cl VIII chlorine ions. It should be especially noted that in the range 11–17 nm, intense lines of chlorine ions are possible, which were not separated due to superposition on the fluorine ions lines. The interpretation of the observed lines was carried out in accordance with [19,20,25] and is given in Table 4.

It is interesting to trace the relative changes in the intensity of the fluorine lines when three different gases are used as a target: CHF<sub>3</sub>, CCl<sub>2</sub>F<sub>2</sub>, SF<sub>6</sub>. These results are presented in Table 5. In the table, all line intensities are normalized to the intensity of the line 13.99 nm (F VII), which makes it possible to take into account different concentrations of fluorine ions in the discharge zone. Based on the presented table, the following conclusions can be drawn.

In case of transition from CHF<sub>3</sub> to CCl<sub>2</sub>F<sub>2</sub> and SF<sub>6</sub>, no pronounced increase in the intensity of the lines corresponding to ions in high ionization degrees (F VII).

For the same lines, in case of transition from CHF<sub>3</sub> to CCl<sub>2</sub>F<sub>2</sub>, changes in the relative intensity of the emission lines are observed. These changes are small, up to 0.3 times.

In case of the transition from CHF<sub>3</sub> to SF<sub>6</sub>, the changes in the relative intensity of the emission lines are more significant — up to 2 times. These changes indicate that the parameters of the laser plasma obtained on CHF<sub>3</sub>, CCl<sub>2</sub>F<sub>2</sub> and SF<sub>6</sub> targets are very close to each other.

## Conclusions

In this article, the emission spectra of a laser-plasma source with gas-jet targets of various molecular gases are studied. These targets were formed using different nozzles at different gas pressures at the nozzle inlet.

1) LPS emission spectra were obtained using various gas targets with various fluorine-containing molecular gases. The obtained spectra were interpreted and the ions emitting in this spectral range were determined. The fluorine lines in the spectra of gas targets of various structures at various gas pressures at the nozzle inlet do not undergo large changes. The maximum ionization degree achieved in our experiment was F VII. As for sulfur and chlorine, the recorded emission spectra are characterized by a small number of lines corresponding to these elements and, accordingly, are of little information. The maximum ionization degrees achieved in our experiment were S VIII, Cl VIII.

2) Changes in the emission spectra were determined when using different nozzles that form jets of different structures at different gas pressures at the nozzle inlet. It is found that with an increase in particle concentration in the spark formation zone, an increase in the intensity of emission lines corresponding to ions of high ionization degrees and, accordingly, an increase in plasma temperature are observed. However, the maximum ionization degree remains the same. Also, with an increase in gas concentrations in the discharge zone, a redistribution of line intensities occurs for an emitting ion of one ionization degree. Thus, using gas targets of various structures and varying the inlet pressure, it is possible to change the intensity of individual emission lines over a wide range. A qualitative change in the spectra requires a sharp increase in the number of particles in the discharge zone, which is possible both due to an increase in pressure at the nozzle inlet and due to an increase in the critical section of the nozzles. To increase plasma temperature and radiation intensity, while minimizing the requirements for the pumping system, it is optimal to use small-section nozzles at high gas pressure at the nozzle inlet [26]. A similar result is also expected in case of transition to liquid targets [27].

3) When using various fluorine-containing gases as targets, in particular, in case of transition from CHF<sub>3</sub> to CCl<sub>2</sub>F<sub>2</sub>, no significant changes in the relative intensities of the lines corresponding to fluorine ions are observed. In case of transition from CHF<sub>3</sub> to SF<sub>6</sub>, no strong changes in the shape of the emission spectrum formed by fluorine ions are observed, but a relative increase in the intensity of individual emission lines is observed. Thus, when using various fluorine-containing gas targets, it is possible to significantly change the intensities of individual lines formed by fluorine ions.

**Table 5.** Relative intensities of fluorine ion lines using various fluorine-containing compounds as targets

Wavelength, nm	Ion	Intensity for different targets		
		CHF <sub>3</sub> Nozzle 450 μm, 3 bar	CCl <sub>2</sub> F <sub>2</sub> Nozzle 450 μm, 3 bar	SF <sub>6</sub> Nozzle 450 μm, 3 bar
9.57	F VII	0.60	0.45	0.66
11.294	F VII	0.97	0.81	0.95
12.21	F VI	0.30	0.31	0.34
12.44	F VI	0.30	0.22	0.36
12.78	F VII	2.61	2.46	–
13.48	F VII	0.58	0.45	0.67
13.99	F VI	1.00	1.00	1.00
14.59	F VI	0.47	0.33	0.59
14.68	F VI	0.80	0.63	0.95
14.87	F VI	0.40	0.34	0.49
15.38	F VI	0.30	0.24	0.38
15.62	F VI	0.34	0.31	0.42
16.35	F VI	0.38	0.41	0.53
19.48	F VII	0.29	0.29	0.50

## Funding

The work was carried out within the scope of State Assignment № 0030-2021-0022 and supported by RFBR grant 20-02-00364.

## Conflict of interest

The authors declare that they have no conflict of interest.

## References

- [1] S.V. Kuzin, V.N. Polkovnikov, N.N. Salashchenko. *Izvestiya RAN. Ser. fiz.*, **75** (1), 88 (2011) (in Russian).
- [2] N.I. Chkhalo, N.N. Salashchenko. *AIP Adv.*, **3** (8), 082130 (2013).
- [3] M.M. Barysheva, A.E. Pestov, N.N. Salashchenko, M.N. Toropov, N.I. Chkhalo. *UFN*, **182** (7), 727 (2012) (in Russian).
- [4] I.V. Malyshev, A.E. Pestov, V.N. Polkovnikov, N.N. Salashchenko, M.N. Toropov, N.I. Chkhalo. *Poverkhnost. Rentgenovskie, sinhrotronnye i nejtronnye issledovaniya* **1**, 3 (2019) (in Russian).
- [5] M. Suzuki, H. Daido, I.W. Choi, W. Yu, K. Nagai, T. Norimatsu, H. Fiedorowicz. *Phys. Plasm.*, **10** (1), 227 (2003).
- [6] M.B. Smirnov, W. Becker. *Phys. Rev. A*, **74** (1), 013201 (2006).
- [7] N.I. Chkhalo, S.A. Garakhin, S.V. Golubev, A.Ya. Lopatin, A.N. Nechay, A.E. Pestov, N.N. Salashchenko, M.N. Toropov, N.N. Tsybin, A.V. Vodopyanov, S. Yulin. *Appl. Phys. Lett.*, **112** (22), 221101 (2018).
- [8] H. Fiedorowicz, A. Bartnik, M. Szczurek, H. Daido, N. Sakaya, V. Kmetik, T. Wilhein. *Opt. Commun.*, **163** (1–3), 103 (1999).
- [9] Y. Tao, M.S. Tillack, K.L. Sequoia, R.A. Burdt, S. Yuspeh, F. Najmabadi. *Appl. Phys. Lett.*, **92** (25), 251501 (2008).
- [10] T. Higashiguchi, T. Otsuka, N. Yugami, W. Jiang, A. Endo, B. Li, G. O'Sullivan. *Appl. Phys. Lett.*, **99** (19), 191502 (2011).
- [11] K. Fukugaki, S. Amano, A. Shimoura, T. Inoue, S. Miyamoto, T. Mochizuki. *Rev. Sci. Instr.*, **77** (6), 063114 (2006).
- [12] B.A. Hansson, O. Hemberg, H.M. Hertz, M. Berglund, H.J. Choi, B. Jacobsson, M. Wilner. *Rev. Sci. Instr.*, **75** (6), 2122 (2004).
- [13] A.N. Nechay, A.A. Perekalov, N.N. Salashchenko, N.I. Chkhalo. *Opt. i spektr.*, **129** (2), 146 (2021) (in Russian).
- [14] A.N. Nechay, A.A. Perekalov, N.N. Salashchenko, N.I. Chkhalo. *Opt. i spektr.*, **129** (3), 266 (2021) (in Russian).
- [15] A.N. Nechay, A.A. Perekalov, N.I. Chkhalo, N.N. Salashchenko. *Opt. i spektr.*, **129** (6), 755 (2021) (in Russian).
- [16] A.N. Nechai, A.A. Perekalov, N.I. Chkhalo, N.N. Salashchenko, I.G. Zabrodin, I.A. Kaskov, A.E. Pestov. *Poverkhnost. Rentgenovskie, sinhrotronnye i nejtronnye issledovaniya* (in Russian) **9**, 83 (2019) (in Russian).
- [17] B. Abel, J. Assmann, M. Faubel, K. Gäbel, S. Kranzusch, E. Lugovoj, C. Peth. *J. Appl. Phys.*, **95** (12), 7619 (2004).
- [18] D.J. Pegg, P.M. Griffin, H.H. Haselton, R. Laubert, J.R. Mowat, R.S. Thoe, I.A. Sellin. *Phys. Rev. A*, **10** (3), 745 (1974).
- [19] R.L. Kelly, L.J. Palumbo. *Atomic and ionic emission lines below 2000 angstroms-hydrogen through krypton* (Naval Research Lab, Washington DC, 1973).
- [20] *NIST Atomic Spectra Database*, Gaithersburg, 2009–2019. <https://www.nist.gov/pml/atomic-spectra-database>.
- [21] B. Edlén. *Z. Phys.*, **94** (1–2), 47 (1935).
- [22] R.E. LaVilla. *J. Chem. Phys.*, **57** (2), 899 (1972).
- [23] H. Fiedorowicz, A. Bartnik, Z. Patron, P. Parys. *Laser and Particle Beams*, **12** (3), 471 (1994).
- [24] L.I. Podobedova, D.E. Kelleher, W.L. Wiese. *J. Phys. and Chem. Ref. Data*, **38** (2), 171 (2009).
- [25] H.G. Berry, J. Desesquelles, K.T. Cheng, R.M. Schectman. *Phys. Rev. A*, **18** (2), 546 (1978).
- [26] M. Müller, T. Mey, J. Niemeyer, M. Lorenz, K. Mann. *AIP Conf. Proc.*, **1764** (1), 030003 (2016).
- [27] B.A.M. Hansson, H.M. Hertz. *J. Phys. D.*, **37** (23), 3233 (2004).